

Exciton escape in CdSe core-shell quantum dots: Implications for the development of nanocrystal solar cells

J. S. de Sousa, J. A. K. Freire, and G. A. Farias

Universidade Federal do Ceará, Departamento de Física, Caixa Postal 6030, 60455-760 Fortaleza, Ceará, Brazil

(Received 9 October 2006; revised manuscript received 21 December 2006; published 23 October 2007)

We investigate the tunneling escape of confined excitons in CdSe core-shell quantum dots by means of the time-dependent Schrodinger equation. Our results indicate that obtaining efficient charge extraction strongly depends on the interplay between parameters such as nanocrystal sizes, shell thicknesses, external electric fields, and confinement barrier heights.

DOI: [10.1103/PhysRevB.76.155317](https://doi.org/10.1103/PhysRevB.76.155317)

PACS number(s): 73.40.Gk, 71.35.-y, 85.30.De

I. INTRODUCTION

It has been suggested that nanocrystals (NC's) may exhibit important ingredients for the development of inexpensive and efficient solar cells because of (i) the possibility of tailoring their bandgap through size and shape control in order to absorb light in the whole solar spectrum and (ii) the enhanced impact ionization caused by the tridimensional confinement that leads to the generation of two (or more) electron-hole pairs (e - h pairs) for each photon absorbed.¹⁻³ In particular, recent experimental observations demonstrated the generation of up to seven excitons with a single photon.⁴⁻⁶

The most probable configurations for the development of NC solar cells seem to be based on (i) tridimensionally ordered array of NC's, in such way that the inter-NC distance is small enough to allow the formation of minibands through electronic coupling between neighboring NC's or (ii) NC's dispersed in organic semiconductor polymer matrices.^{7,8} Nowadays, CdSe colloidal NC's can be inexpensively grown with precise control over their shape and size.⁹ However, the environment where NC's are embedded strongly affects their electronic structure and optical properties.^{10,11} Chemically passivating the NC core with a thin shell of wide bandgap semiconductor prevents chemical interaction with the inter-NC environment. Moreover, it allows substantial improvement of their optical stability and exhibits greater tolerance to processing conditions necessary for incorporation into solid state structures.

Several wide band gap semiconductors (e.g., ZnS, CdS, ZnSe) have been epitaxially grown on the surface of CdSe colloidal NC's.^{12,13} Regardless the shell material, incident photons are absorbed by the NC's, generating single or multiple electron-hole (e - h) pairs. There are some possible relaxation channels for these excited NC's: (i) radiative recombination emitting photons with energies that inversely scale with the NC sizes, (ii) nonradiative recombination through Auger processes or phonon emission,¹⁴ (iii) quantum tunneling through the shell layer, and temperature related effects such as (iv) thermionic emission and (v) thermal assisted tunneling.^{15,16} Depending on the relative efficiencies of such channels, different NC-based applications can be developed. For instance, faster radiative transitions in comparison to other processes lead to light emitting applications, while efficient escape of e - h pairs may generate electrical currents,

which are useful for the development of photovoltaic devices. In this work, the out-tunneling of e - h pairs occupying the ground state of CdSe core-shell quantum dots (QD's) is addressed. We remark that the extraction of carriers by quantum tunneling is a well known mechanism in low-dimensional photovoltaic devices.

II. PHYSICAL MODELING

The photogenerated current in NC solar cells arises from the fraction of e - h pairs created by the absorption of photons that escape from the QD's through the shell layer before recombining either radiatively or not. For simplicity, we focus on the escape dynamics of a single e - h pair. Other electronic processes occurring outside QD's are disregarded. The main escape processes are depicted in Fig. 1. Due to the discreteness of the density of states, the energy difference between adjacent states in the conduction and valence bands is larger than the thermal activation energy $k_B T$ even at room temperature, suppressing the occupation of excited states. This is particularly important in CdSe QD's because of the small carrier effective masses. In the case of small confinement barriers, the enhanced binding energy in QD's is several times larger than $k_B T$, so that temperature effects are not strong enough to dissociate confined e - h pairs. Thus, temperature related processes can be ruled out and the main contribution to the photogenerated current can be considered as arising from the out-tunneling of ground state e - h pairs. There are two obstacles competing to the out-tunneling of this e - h pair: shell barrier and Coulomb interaction. If these mechanisms are strong enough to hold the confined e - h pair during times of the same order of the recombination lifetime, the conversion efficiency are expected to be very low.

In order to simulate the dynamics of a single ground state e - h pair in the system shown in Fig. 1, we solve the time-dependent Schrodinger equation

$$H_T \Psi_T(\mathbf{r}_e, \mathbf{r}_h; t) = i\hbar \frac{\partial \Psi_T(\mathbf{r}_e, \mathbf{r}_h; t)}{\partial t}, \quad (1)$$

where $\Psi_T(\mathbf{r}_e, \mathbf{r}_h; t)$ is the total e - h pair wave function. The two-particle Hamiltonian is given by

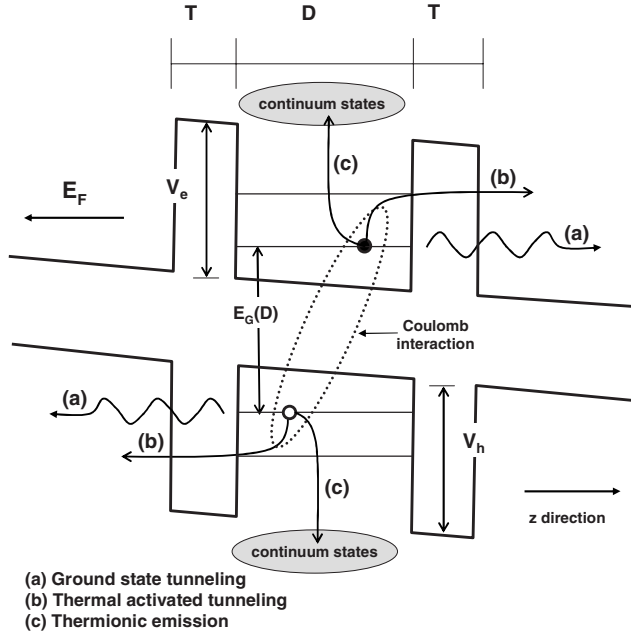


FIG. 1. Schematics of the escape processes of an e - h pair in a single QD. T and D represent the shell thickness and core size of the QD, respectively. The conduction and valence band energy barriers are represented by V_e and V_h , respectively, and E_F is an external electric field. The figure shows the processes responsible for current generation observed in photovoltaic devices: (a) Ground-state tunneling, (b) thermal assisted tunneling, and (c) thermionic emission. Processes (b) and (c) are highly dependent on temperature (Refs. 15 and 16).

$$H_T = \sum_{i=e,h} \left[-\frac{\hbar^2}{2} \nabla \frac{1}{m_i^*(\mathbf{r}_i)} \nabla + V_i(\mathbf{r}_i) \right] - \frac{q^2}{4\pi\epsilon} \frac{1}{|\mathbf{r}_e - \mathbf{r}_h|}, \quad (2)$$

where $i=(e,h)$ denotes the carrier type, $m_i^*(\mathbf{r}_i)$ is the position-dependent effective mass, and $V_i(\mathbf{r}_i)$ represents the confinement potential of each carrier type. Figure 1 also shows that the QD's are subject to an external electric field E_F in the z direction, which may be created by the external electrodes of the photovoltaic device. We assume that this electric field gives a preferential direction of tunneling, in such a way that carriers tunneling in the other directions can be disregarded. This assumption allows to decouple the six-variable Schrodinger equation in two problems: one equation to describe the carriers behavior in the z direction and another one for the xy plane.

The overall strategy to solve the present time-dependent problem is depicted in Fig. 2. Before solving Eq. (1), the time-independent equation $H_T \Psi_T(\mathbf{r}_e, \mathbf{r}_h) = E_T \Psi_T(\mathbf{r}_e, \mathbf{r}_h)$ is solved for an e - h pair confined in a fully bound potential profile. The resulting e - h state $\Psi_T(\mathbf{r}_e, \mathbf{r}_h)$ is used as initial condition for the time evolution in the quasibound system shown in Fig. 1. Details about the solution of the time-independent and time-dependent equations are discussed in the next subsections.

A. Time-independent Schrodinger equation: Confined excitons

In order to avoid the solution of a six-variable Schrodinger equation, we conveniently write the confinement po-

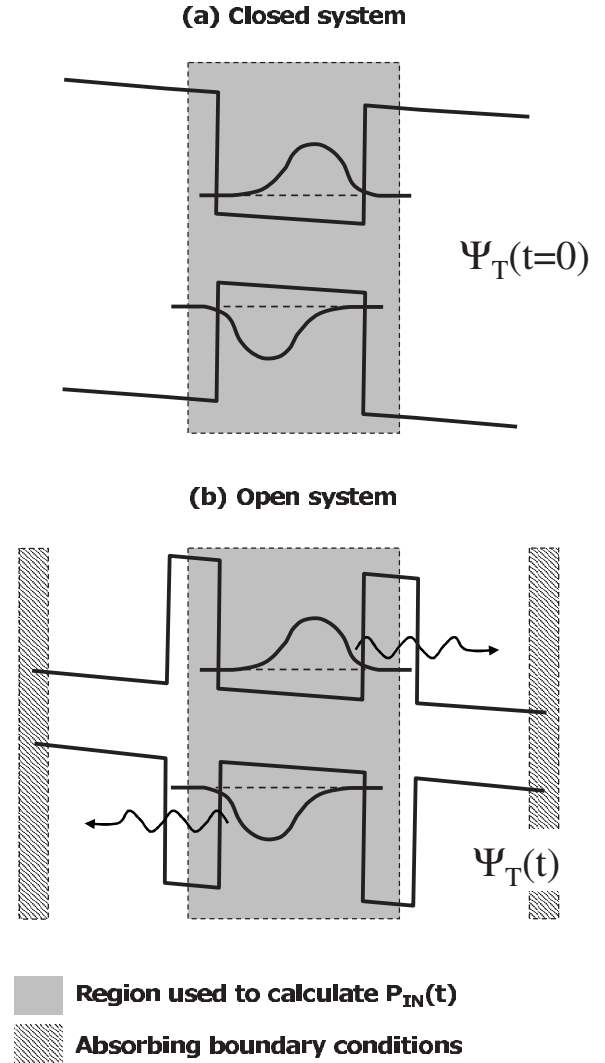


FIG. 2. Overview of the strategy adopted for solving the time-dependent Schrodinger equation. First, we solve the time-independent Eq. (5) with a closed confinement potential (a) to obtain $\Psi_T(t=0)$. Then, we solve Eq. (9) with a quasibound confinement potential (b) using $\Psi_T(t=0)$ as initial condition. Absorbing boundary conditions are used at the edges of the computational mesh to avoid WF reflections which would affect the calculation of the tunneling time (Ref. 17).

entials as $V_i(\mathbf{r}_i) = V_z^{(i)}(z_i) + V_{\perp}^{(i)}(\mathbf{r}_{\perp,i})$, where $\mathbf{r}_{\perp,i}$ denotes the i th particle position in the plane perpendicular to the z_i direction. This assumption allows H_T to be written as $H_T = H_z^{(e)} + H_{\perp}^{(e)} + H_z^{(h)} + H_{\perp}^{(h)} + V_{eh}$, where $H_z^{(i)}$ and $H_{\perp}^{(i)}$ represent the individual carrier Hamiltonians in the z and perpendicular directions, respectively. V_{eh} represents the Coulomb interaction between the carriers. This separation is not suitable for spherical confinement potentials. The Schrodinger equation in the perpendicular direction is

$$H_{\perp}^{(i)} \phi_i(\mathbf{r}_{\perp,i}) = E_{\perp}^{(i)} \phi_i(\mathbf{r}_{\perp,i}). \quad (3)$$

Thus, total wave function (WF) can be written as

$$\Psi_T(\mathbf{r}_e, \mathbf{r}_h) = \psi(z_e, z_h) \phi_e(\mathbf{r}_{\perp,e}) \phi_h(\mathbf{r}_{\perp,h}). \quad (4)$$

By multiplying the time-independent equation $H_T \Psi_T(\mathbf{r}_e, \mathbf{r}_h) = E_T \Psi_T(\mathbf{r}_e, \mathbf{r}_h)$ at left by $\phi_e(\mathbf{r}_{\perp,e}) \phi_h(\mathbf{r}_{\perp,h})$ and integrating in the coordinates $\mathbf{r}_{\perp,e}$ and $\mathbf{r}_{\perp,h}$, we obtain a Schrödinger equation involving only the z_i coordinates

$$H_z^{\text{eff}} \psi(z_e, z_h) = E_z \psi(z_e, z_h), \quad (5)$$

where

$$H_z^{\text{eff}} = H_z^{(e)} + H_z^{(h)} + V_z^{\text{eff}}(z_e, z_h), \quad (6)$$

$$V_z^{\text{eff}}(z_e, z_h) = -\frac{q^2}{4\pi\epsilon} \int \frac{|\phi_e(\mathbf{r}_{\perp,e})|^2 |\phi_h(\mathbf{r}_{\perp,h})|^2}{|\mathbf{r}_e - \mathbf{r}_h|} d\mathbf{r}_{\perp,e} d\mathbf{r}_{\perp,h}. \quad (7)$$

Thus, the original six-variable time-independent problem $H_T \Psi_T(\mathbf{r}_e, \mathbf{r}_h) = E_T \Psi_T(\mathbf{r}_e, \mathbf{r}_h)$ is decoupled into a set of three two-variable equations given by Eqs. (3) and (5), with the total energy E_T given by

$$E_T = E_{\perp}^{(e)} + E_{\perp}^{(h)} + E_z. \quad (8)$$

This decoupling allows to solve Eqs. (3) and (5) separately. The latter equation captures the interplay among external electric fields, Coulomb interaction, and exciton confinement and escape in the direction that the out-tunneling effectively occurs, while the former equation reinforces the full tridimensional confinement characteristic of the problem. From the computational point of view, this is much simpler than solving a full six-variable problem similar to Eq. (1). However, further simplifications are still possible: one may consider potential profiles $V_i(\mathbf{r}_{i\perp})$ with known analytical solutions for the Schrödinger equations Eqs. (3), say square or circular confinement barriers either finite or infinite confinement barriers. Thus, we only have to solve Eq. (5), which can be easily done by regular finite difference methods. We remark that the calculation of the effective Coulomb potential in Eq. (7) presents a discontinuity, and the strategy for dealing with this problem is outlined in Ref. 18.

B. Time-dependent Schrödinger equation: Exciton escape

As the exciton escape occurs in the z direction, we solve a simpler form of the time-dependent Schrödinger equation

$$H_z^{\text{eff}} \psi(z_e, z_h; t) = i\hbar \frac{\partial \psi(z_e, z_h; t)}{\partial t}, \quad (9)$$

following the computational scheme described in Refs. 19 and 20. The out-tunneling time of the e - h pair is computed as follows. At each time-step, the probability of the e - h pair to be inside the QD can be evaluated using

$$P_{\text{in}}(t) = \int_{\text{QD}} |\Psi_T(\mathbf{r}_e, \mathbf{r}_h; t)|^2 d\mathbf{r}_e d\mathbf{r}_h. \quad (10)$$

The tunneling time τ_T of the e - h pair is estimated through the fit of the $P_{\text{in}}(t)$ curve with a single exponential decaying curve such as $A \exp(-t/\tau_T)$. The out-tunneling time is obtained for an e - h pair occupying the ground state. This ap-

TABLE I. Compilation of the material parameters used in this work. The parameters not shown are not necessary to the model.

Param.	CdSe	CdS	ZnS
a_0 (Å)	6.052 ^a	5.7982 ^a	5.3476 ^a
C_{11} (GPa)	66.7 ^b	85.2 ^c	106.7 ^c
C_{12} (GPa)	46.3 ^b	54.5 ^c	66.6 ^c
E_g (eV)	1.74 ^d	2.58 ^e	3.84 ^e
a_c (eV)		-3.59 ^a	-6.02 ^a
a_v (eV)		0.92 ^e	1.83 ^e
b (eV)		-1.18 ^e	-1.39 ^e
$V_e^{(0)}$ (eV)		0.32 ^f	1.44 ^f
$V_h^{(0)}$ (eV)		0.42 ^f	0.60 ^f
m_e/m_0	0.13	0.20	0.367
m_{hh}/m_0	0.45	0.80	0.569
ϵ/ϵ_0	9.1		

^aReference 23.

^bReference 24.

^cReference 25.

^dReference 26.

^eReference 27.

^fReference 28.

^gReference 29.

proach was used previously to investigate the lifetime of quasibound states in open quantum structures.^{21,22}

Among all materials used to cover CdSe NC's, we will focus on CdS and ZnS because they exhibit the lowest and highest confinement energy barriers with respect to the CdSe core, respectively. Thus, any other shell material is expected to present an intermediate behavior between CdS and ZnS. The materials parameters used in this work are given in Table I.

C. Effects of lattice mismatch strain

Strain related effects are expected due to the different lattice parameters of CdSe, CdS, and ZnS. Strain affects QD properties by modifying the spatial confinement profile and/or the height of confinement barriers. In the case of CdSe/CdS, the lattice mismatch is relatively small (about 4%), and the coherent epitaxial growth of the CdS shell on CdSe has been reported.^{30,31} As for ZnS/CdSe QD's, Hines *et al.* reported that the capping process does not lead to significant modifications of the optical properties.³² In particular, the first exciton peak becomes broadened but it is not shifted appreciably. Only at shorter wavelength the absorption spectrum deviate significantly from the uncapped QD, suggesting that the first electronic states of the CdSe core are weakly modified. In fact, the low lattice mismatch requirement for epitaxial growth of a shell layer on the surface of colloidal QD's is not as stringent as in two-dimensional systems because the total area over which the strain accumulates is small. It is expected that strain becomes more important in very long rodlike QD's because they exhibit an average curvature that is intermediate between the surface of a spherical QD and a flat film.³³ In principle, these results could lead us

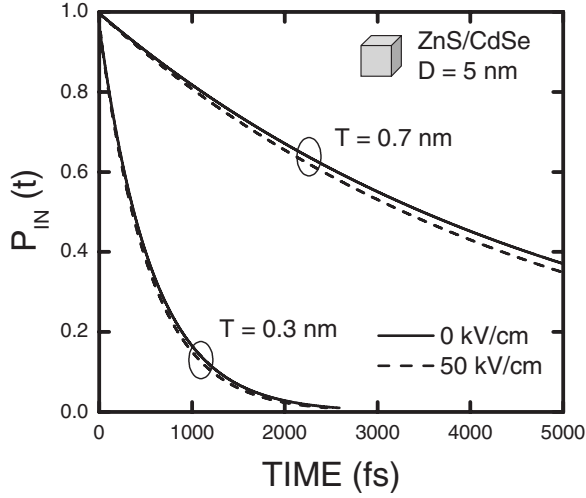


FIG. 3. Time dependence of the probability $P_{in}(t)$ to find the $e-h$ pair within the QD. The curves represent a cubic ZnS/CdSe QD of 5 nm with infinite lateral confinement barriers. Shell thicknesses of $T=0.3$ nm and $T=0.7$ nm and electrical fields of $E_F=0$ kV/cm and $E_F=50$ kV/cm were used. The Coulomb interaction is not considered in this particular case.

to conclude that strain does not play a significant role on τ_T . However, it is known that the lifetime of quasibound states is very sensitive to the height of the confinement barriers. Therefore, strain effects must be investigated.

Based on the assumption of the one-dimensional out-tunneling, we only account for strain effects in this direction. For simplicity, we assume the out-tunneling occurs along [001] direction, for which the confinement potentials with respect to the barriers without strain can be written as²⁵

$$V_e = V_e^{(0)} + a_c(\epsilon_{xx} + \epsilon_{yy} + \epsilon_{zz}), \quad (11)$$

$$V_h = V_h^{(0)} - a_v(\epsilon_{xx} + \epsilon_{yy} + \epsilon_{zz}) \pm b(\epsilon_{zz} - \epsilon_{xx}), \quad (12)$$

where $V_{e,h}^{(0)}$ are the unstrained confinement barriers, a_c and a_v are the hydrostatic deformation potentials for conduction and valence bands, respectively, and b is the shear deformation potential. The \pm sign refers to the confinement potential of the heavy and light holes, respectively. In this work, our investigation will focus exclusively on the ground state heavy-hole exciton. The components of strain tensor are given by $\epsilon_{xx} = \epsilon_{yy} = (a_{||} - a_0)/a_0$, $\epsilon_{zz} = -2C_{12}/C_{11}\epsilon_{xx}$, where $a_{||}$ is the in plane lattice constant and a_0 is the equilibrium lattice constant. C_{ij} represent the elastic coefficient. These parameters are shown in Table I.

III. RESULTS

Because of the finite shell thickness, the confined carriers tend to tunnel out and the probability to find the $e-h$ pair within the QD decreases as time evolves. Figure 3 displays the time dependence of the probability to find the $e-h$ pair within the QD given by Eq. (10). One notices that at initial instant $t=0$, the $e-h$ pair is entirely confined within the QD. For the ZnS/CdSe QD with shell thickness of $T=0.3$ nm, the

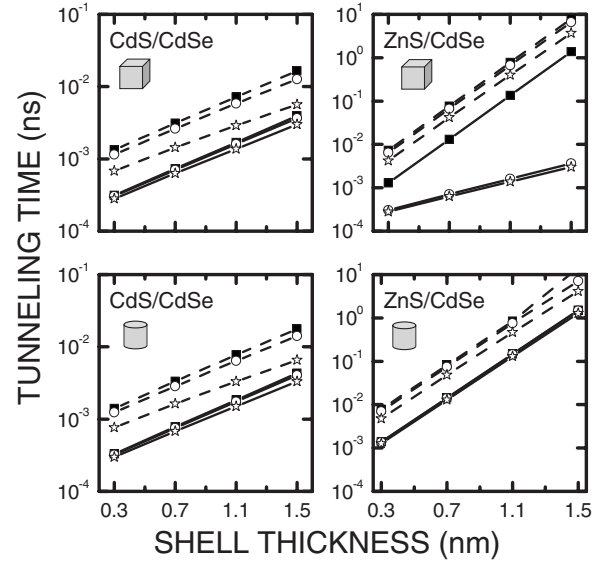


FIG. 4. Shell thickness dependence of the out-tunneling time of $e-h$ pairs confined in CdS/CdSe (left) and ZnS/CdSe (right) QD's with core sizes of 5 nm (solid lines) and 10 nm (dashed lines). Two different QD shapes are used: squared box (top) and cylindrical (bottom). The influence of external electric fields is also displayed: 0 kV/cm (square), 50 kV/cm (circle), 100 kV/cm (star).

$e-h$ pair completely escapes after 2000 fs. In the case of $T=0.7$ nm, there is approximately 40% of chance to find the $e-h$ pair in the QD after 5000 fs. Our simulations are in good agreement with the fact that the thicker the tunneling barrier, the smaller the transmission coefficient. In addition, all curves exhibit a single exponential behavior, which supports the validity of our fitting procedure to calculate the out-tunneling times. In the presence of electric fields, the confined carriers tunnel out towards opposite directions along the electric field direction. Otherwise, both carriers tunnel radially out of the QD without any preferred direction. As our model presumes the out-tunneling in a single direction, the out-tunneling times calculated without the presence of electric fields are a little overestimated.

Figure 4 compares the calculated shell thickness dependence of the exciton tunneling time in both CdS/CdSe and ZnS/CdSe core-shell QD's for different electric field strengths, QD sizes, and shape. The range of shell thickness investigated is representative of current state-of-art core-shell QD's.^{12,13} The out-tunneling times in CdS/CdSe QD's are few orders of magnitude faster than in ZnS/CdSe ones because of their lower confinement barriers. One also notices that the estimated tunneling times in CdS/CdSe QD's are much below the nanosecond time scale regardless the shell thickness, electric field, QD shape and size. On the other hand, the out-tunneling times in ZnS/CdSe QD's become of the order of nanoseconds for the combination of QD sizes in the range $D=5-10$ nm and shell thicknesses between 1.0 and 1.5 nm, regardless the QD shape. As for the electric fields, they tend to separate $e-h$ pairs, decreasing the out-tunneling times. However, their effect is almost negligible for small QD's because of the tight confinement imposed to the $e-h$ pairs. This is not true for reasonably large QD's be-

TABLE II. Comparison of the tunneling time with (τ_T) and without (τ_{NC}) the Coulomb interaction for QD's with different shape, sizes, and applied electric fields. For comparison, the total exciton energies (E_T) and binding energies (E_B) are also displayed. The shell material is ZnS with 0.7 nm of thickness.

Shape	E_F (kV/cm)	D (nm)	E_T (eV)	E_B (eV)	τ_T (10^{-2} ns)	τ_{NC} (10^{-2} ns)
Box	0	5	1.996	0.116	1.32	0.505
		10	1.764	0.068	7.67	3.600
Cylinder	0	5	1.989	0.123	1.43	0.505
		10	1.759	0.073	8.24	3.600
Box	50	5	1.995	0.1160	1.28	0.476
		10	1.762	0.0638	6.68	2.454
Cylinder	50	5	1.989	0.1224	1.41	0.476
		10	1.758	0.0681	7.42	2.454

cause larger volumes exhibit smaller binding energies, which eases the separation of the e - h pair. For instance, τ_T in a 10 nm wide QD is a half-order magnitude smaller when $E_F = 100$ kV/cm in comparison to the ones calculated without E_F .

In addition to the shell thickness, the QD size is also important for the determination of the exciton tunneling time. For a given shape, the comparison of τ_T in QD's with different sizes indicates that it inversely scales with D . Within a classical point of view, the larger the energy of individual confined carriers the faster they move back and forth within the QD, hitting the confinement barriers and increasing their tunneling probability. As the confined carriers energy scales with the QD size as $E_T \propto D^{-n}$, where $n=2$ ($n < 2$) for infinite (finite) confinement barriers, small QD's must exhibit faster exciton tunneling times. Moreover, the tunneling time is much more sensitive to variations in the shell thickness than in the QD size. Figure 4 also shows that shape matters only for certain cases. By keeping other parameters unchanged, it is not observed any significant difference in the tunneling time in CdS/CdSe QD's with different shapes. This is also true for ZnS/CdSe ones, except for the cases where $D=5$ nm and $E_F \neq 0$ kV/cm (cubic QD's). Actually, the tunneling times in cylindrical QD's are a little larger than in cubic QD's. This sounds contradictory because the smaller volume of cylindrical QD's leads to larger exciton energies, which are expected to yield faster tunneling times, at least when comparing QD's of the same shape. The reason for this apparent contradiction relies on the exciton binding energy, which is slightly larger for cylindrical QD's in comparison to cubic ones. The comparison between τ_T and τ_{NC} , where τ_{NC} represents the tunneling time calculated without the Coulomb interaction, is shown in Table II. One can see that calculations without the Coulomb interaction lead to tunneling times that are significantly faster. Depending on the shell thickness the difference between τ_T and τ_{NC} can be larger than one order of magnitude.

Finally, we also investigated the role of strain. We did not observe any significant change in the exciton energies with

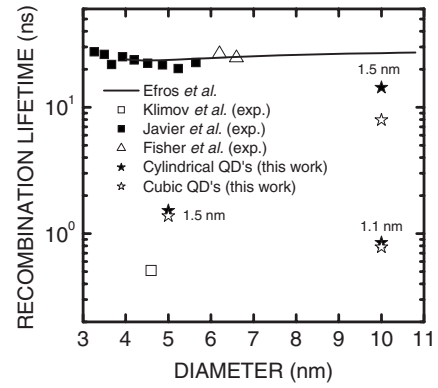


FIG. 5. Comparison of the exciton tunneling times (stars) in ZnS/CdSe QD's with the recombination lifetimes in CdSe QD's obtained from Efron *et al.* (solid line) (Ref. 35), Klimov *et al.* (open square) (Ref. 14), Javier *et al.* (solid square) (Ref. 36), and Fisher *et al.* (open triangle) (Ref. 37). Our calculations were performed for QD sizes of 5 nm and 10 nm with different shapes (cylindrical: solid stars, cubic: open stars) and shell thicknesses (1.1 nm and 1.5 nm, as indicated in the figure).

respect to the case without strain, which is consistent with the experimental results of other groups.³⁰⁻³³ As for the out-tunneling times, we observed an average increase of 20% (3%) for diameters of 5 nm (10 nm) and $E_F=50$ kV/cm. Since these changes occur within the same order of magnitude (10^{-2} ns), they can be also considered very small. In the context of material systems studied here, this is caused by the fact that the reduction of the confinement potential in the conduction band is compensated by an increase of the heavy-hole confinement potential in the valence band.

IV. DISCUSSION

In order to identify the ideal conditions for which QD solar cells are able to work, it is necessary to compare the exciton tunneling times with their recombination lifetimes. Theoretically, the radiative recombination lifetime τ_j of an e - h state $|j\rangle$ to the ground state $|0\rangle$ can be computed with $\tau_j = \Gamma_j^{-1}$, where Γ_j^{-1} is the recombination rate of this transition.³⁴ Γ_j depends on the complicated details of CdSe valence band structure. It is known that the combination of the intrinsic crystal/shape anisotropy and confinement-enhanced electron-hole exchange degeneracy lifts the spin degeneracy of the band-edge exciton into three sets with net spin projections $J=0, 1, 2$. The ground state ($J=2$) is optically inactive because $\Gamma_{J=2}=0$, leading to infinite radiative recombination lifetimes, and the lowest optically active exciton state is $J=1$.³⁵

Figure 5 displays the size-dependence of the radiative recombination lifetime of excitons in CdSe QD's. The experimental values were collected from the literature.^{14,36,37} The solid line represents the recombination lifetime of the bright exciton state ($J=1$) in spherical QD's, with infinite confinement barriers, calculated with the model presented in Ref. 35. Depending on the QD size and shell thickness, these quantities range in the same order of magnitude. Due to the proba-

bilistic nature of the electronic transitions, the faster the tunneling times, the more efficient will be the conversion of light into electrical currents. The confinement barriers height is also an important parameter. For example, the tunneling time in CdS/CdSe QD's varies in the range 10^{-3} – 10^{-2} ns, which is too low to appear in the scale of Fig. 5. This suggests that CdS/CdSe QD's are good candidates for NC based solar cells. However, they are not as chemically stable as ZnS/CdSe ones.¹² In addition to the QD size, surface passivation and thermal activation between dark and higher-lying bright exciton states are other important factors affecting the exciton recombination lifetime.^{32,34,38,39} For example, the recombination data from Klimov *et al.* presented in Fig. 5 is nearly one order of magnitude smaller than the other experimental data shown.¹⁴ In this case, the recombination lifetime is smaller than the tunneling time in ZnS/CdSe QD's with $D=5$ nm and $T=1.5$ nm, indicating that the NC solar cells for this combination of QD parameters may not work. Moreover, depending on the QD size and shell thickness, τ_T can be of the same order of the relaxation time of multiple $e-h$ pairs by means of Auger recombination. For example, Klimov *et al.* reported that τ_2 (relaxation time from 2 to 1 $e-h$ pair) in a 8.2 nm QD is 0.363 ns,¹⁴ which is much slower than the $\tau_T=0.0742$ ns in a 10 nm cylindrical QD (see Table II). This suggests that multiple $e-h$ pairs might be converted into electrical currents practically without loss.⁴⁻⁶ Of course, in QD's containing two $e-h$ pairs, the Coulomb potential acting on each particle has three contributions, two attractive and a repulsive one. Therefore, we expect that the out-tunneling time of one of the confined $e-h$ pairs be either of the same order of magnitude or slightly smaller than τ_T .

Despite the fact that the theoretical model presented in Sec. II is not able to deal with spherical QD's, the interplay between shape and Coulomb interaction discussed in Sec. III allows us to predict some trends about the behavior of τ_T in spherical QD's. Because of their larger binding energies in comparison to cylindrical ones, they will exhibit slower tunneling times, becoming even closer to the experimental recombination lifetimes. Concerning the use of infinite confinement barriers in the perpendicular directions, it is also possible to draw some comments. First, they lead to smaller binding and total exciton energies. These quantities scale directly (inversely) with τ_T such that their dependence will nearly cancel each other.

V. CONCLUDING REMARKS

In conclusion, we performed a theoretical investigation of the out-tunneling of $e-h$ pairs from CdSe based core-shell QD's through time-dependent solutions of the Schrodinger equation including the Coulomb interaction. The exciton tunneling times are extremely sensitive to QD sizes, shell thickness and confinement barrier heights. Depending on the combination of these quantities, the out-tunneling times can be comparable to the recombination lifetimes, indicating that achieving efficient charge extraction depends on a careful selection of geometrical parameters. We have also shown that the Coulomb interaction plays an important role on the exciton escape, thus should not be neglected. In our calculations, we considered the perfect alignment between the band edges of the NC core and host material. However, this is an important issue which is also expected to influence the exciton escape. Finally, we focused on the dynamics of single $e-h$ pairs until they tunnel out. Once released, they will either recombine or undergo multiple trapping and escape events from another QD's until they reach the device electrodes. We also remark that even though $e-h$ pairs are able to tunnel out without external electric fields, it does not mean that NC solar cells might work without them. External electric fields drive the separated $e-h$ pair towards the device electrodes. The physical processes governing the charge transport outside the QD's and the geometrical design of the device are also very important for the successful development of NC solar cells. These topics will be dedicated to future investigations.

ACKNOWLEDGMENTS

The authors acknowledge V. N. Freire for the critical reading of this manuscript. J. S. de Sousa is indebted to the Brazilian National Research Council (CNPq) for the financial support through CNPq/CT-ENERG and FUNCAP/CNPq/PPP Grant Nos. 504330/2003-9 and 1015/06, respectively. This work was also supported by CNPq/FUNCAP/PRONEX Grant No. 883103 and the Research Network NanoBiostructures Grant No. 555183/2005-0.

¹A. J. Nozik, *Physica E (Amsterdam)* **14**, 115 (2002).

²M. Califano, A. Zunger, and A. Franceschetti, *Nano Lett.* **4**, 525 (2004).

³M. Califano, A. Zunger, and A. Franceschetti, *Appl. Phys. Lett.* **84**, 2409 (2004).

⁴R. D. Schaller and V. I. Klimov, *Phys. Rev. Lett.* **92**, 186601 (2004).

⁵R. J. Ellingson, M. C. Beard, J. C. Johnson, P. Yu, O. I. Micic, A. J. Nozik, A. Shabaev, and A. L. Efros, *Nano Lett.* **5**, 865 (2005).

⁶R. D. Schaller, M. Sykora, J. M. Pietryga, and V. I. Klimov, *Nano Lett.* **6**, 424 (2006).

⁷W. U. Huynh, J. J. Dittmer, and A. P. Alivisatos, *Science* **295**,

2425 (2002).

⁸M. Gratzel, *Nature (London)* **414**, 338 (2001).

⁹X. Peng, L. Manna, W. Yang, J. Wickham, E. Scher, A. Kadavanchi, and A. P. Alivisatos, *Nature (London)* **404**, 59 (2000).

¹⁰Z. Yu, L. Guo, T. Krauss, and J. Silcox, *Nano Lett.* **5**, 565 (2005).

¹¹I. Mekis, D. V. Talapin, A. Kornowski, M. Haase, and H. J. Weller, *J. Phys. Chem. B* **107**, 7454 (2003).

¹²D. V. Talapin, I. Mekis, S. Gotzinger, A. Kornowski, O. Benson, and H. J. Weller, *J. Phys. Chem. B* **108**, 18826 (2004).

¹³B. O. Dabbousi, J. Rodriguez-Viejo, F. V. Mikulec, J. R. Heine, H. Mattoussi, R. Ober, K. F. Jensen, and M. G. Bawendi, *J. Phys. Chem. B* **101**, 9463 (1997).

- ¹⁴V. I. Klimov, A. A. Mikhailovsky, D. W. McBranch, A. C. Leatherdale, and M. G. Bawendi, *Science* **287**, 1011 (2000).
- ¹⁵N. E. I. Etteh and P. Harrison, *Physica E (Amsterdam)* **13**, 381 (2002).
- ¹⁶J. Appenzeller, M. Radosavljevic, J. Knoch, and Ph. Avouris, *Phys. Rev. Lett.* **92**, 048301 (2004).
- ¹⁷D. Neuhasuer and M. Baer, *J. Chem. Phys.* **90**, 4351 (1989).
- ¹⁸J. R. Chelikowsky, N. Troullier, K. Wu, and Y. Saad, *Phys. Rev. B* **50**, 11355 (1994).
- ¹⁹M. H. Degani, *Appl. Phys. Lett.* **59**, 57 (1991).
- ²⁰M. H. Degani, *Phys. Rev. B* **66**, 233306 (2002).
- ²¹C. L. N. de Oliveira, J. S. de Sousa, J. A. K. Freire, G. A. Farias, V. N. Freire, and M. H. Degani, *Phys. Status Solidi C* **2**, 3031 (2005).
- ²²M. H. Degani, G. A. Farias, and F. M. Peeters, *Phys. Rev. B* **72**, 125408 (2005).
- ²³S-H. Wei and A. Zunger, *Phys. Rev. B* **60**, 5404 (1999).
- ²⁴S. Schulz and G. Czycholl, *Phys. Rev. B* **72**, 165317 (2005).
- ²⁵C. G. Van de Walle, *Phys. Rev. B* **39**, 1871 (1989).
- ²⁶Y. D. Kim, M. V. Klein, S. F. Ren, Y. C. Chang, H. Luo, N. Samarth, and J. K. Furdyna, *Phys. Rev. B* **49**, 7262 (1994).
- ²⁷A. Qteish and R. J. Needs, *Phys. Rev. B* **45**, 1317 (1992).
- ²⁸B. S. Kim, M. A. Islam, L. E. Brus, and I. P. Herman, *J. Appl. Phys.* **89**, 8127 (2001).
- ²⁹Z. Yu, J. Li, D. B. O'Connor, L.-W. Wang, and P. F. Barbara, *J. Phys. Chem. B* **107**, 5670 (2003).
- ³⁰J. J. Li, Y. A. Wang, W. Guo, J. C. Keay, T. D. Mishima, M. B. Johnson, and X. Peng, *J. Am. Chem. Soc.* **125**, 12567 (2003).
- ³¹D. V. Talapin, R. Koeppel, S. Gotzinger, A. Kornowski, J. M. Lupton, A. L. Rogach, O. Benson, J. Feldmann, and H. Weller, *Nano Lett.* **3**, 1677 (2003).
- ³²M. A. Hines and P. Guyot-Sionnest, *J. Phys. Chem.* **100**, 468 (1996).
- ³³L. Manna, E. C. Scher, L.-S. Li, and A. P. Alivisatos, *J. Am. Chem. Soc.* **124**, 7136 (2002).
- ³⁴A. F. van Driel, G. Allan, C. Delerue, P. Lodahl, W. L. Vos, and D. Vanmaekelbergh, *Phys. Rev. Lett.* **95**, 236804 (2005).
- ³⁵A. L. Efros, M. Rosen, M. Kuno, M. Nirmal, D. J. Norris, and M. Bawendi, *Phys. Rev. B* **54**, 4843 (1996).
- ³⁶A. Javier, D. Magana, T. Jennings, and G. F. Strouse, *Appl. Phys. Lett.* **83**, 1423 (2003).
- ³⁷B. R. Fisher, H.-J. Eisler, N. E. Stott, and M. G. Bawendi, *J. Phys. Chem. B* **108**, 143 (2004).
- ³⁸S. A. Crooker, T. Barrick, J. A. Hollingsworth, and V. I. Klimov, *Appl. Phys. Lett.* **82**, 2793 (2003).
- ³⁹O. Labeau, P. Tamarat, and B. Lounis, *Phys. Rev. Lett.* **90**, 257404 (2003).